Available online at www.sciencedirect.com
SCIENCE DIRECT
Dyes and Pigments 73 (2007) 90–97
DYES and PIGMENTS
www.elsevier.com/locate/dyepig

Kinetics of the oxidative decolorization of Reactive Blue-19 by acidic bromate in homogeneous and heterogeneous media

Ali H. Gemeay*, Gehad R. El-Ghrabawy, Ahmed B. Zaki

Department of Chemistry, Faculty of Science, Tanta University, Tanta, Egypt

Received 30 May 2005; received in revised form 11 July 2005; accepted 20 October 2005
Available online 10 January 2006

Abstract

The kinetics of the oxidative decolorization of Reactive Blue dye (C.I. 19) (RB-19) with $KBrO_3$ acidified by both the H_2SO_4 and cation-exchange resins (H^+-form) were followed up by monitoring the decrease of the absorbance of RB-19 at $\lambda_{max} = 592$ nm. In homogenous medium, the reaction was carried out under pseudo-first-order conditions. The $[BrO_3^-]$ was ca 600 greater than that of [RB-19]. The rate of reaction increased with decreasing $[H_2SO_4]$ and $[BrO_3^-]$, while it decreased with increasing [RB-19]. The effects of the ions, Cl^-, Br^-, Mo(IV), and SO_4^{-2} were investigated and the reaction rate increased with increasing concentrations of the former three, while it decreased with increasing $[SO_4^{2-}]$. In heterogeneous medium the reaction exhibited the zero-order kinetics with respect to [RB-19]. The homogeneous system gave a higher rate compared with the heterogeneous one. The reaction is entropy controlled. A reaction mechanism has been proposed.

Keywords: Reactive Blue-19; Reactive dye; Oxidative decolorization; Acidified bromate

1. Introduction

Wastewater treatment is one of the major problems facing the chemical, petrochemical, pharmaceutical, and textile industries. These industries generate large quantities of organic pollutants that cause environmental and health problems. For solving these problems different techniques were applied, e.g. adsorption, oxidation, reduction, electrochemical and membrane filtration. Oxidation processes are widely used both in industrial preparations and in environmental treatments [1,2]. In the textile industry these processes are used for degrading and removing color from dye baths which allow wastewater reuse [3–6]. The oxidation of organic dyes has attracted much attention in recent years [7–11]. Many attempts have been carried out to study the non-catalyzed [12–16], catalyzed [17–23], photocatalyzed [24–28], and electrochemical oxidation of various categories of organic dyes using different oxidizing agents as model systems. Among these oxidants, the acidified potassium bromate with redox potential of 1.5 eV at 25 °C, exhibited temporal behavior depending on the nature of the reductant. Owing to the in situ generation of reactive intermediates of various oxidation states of bromine in the presence of acidic bromate, the reducing substrates undergo complex reactions and exhibit linear and non-linear dynamic behaviors [29–32].

The oxidation of organic dyes with potassium bromate in acidic medium has attracted much attention. The oxidation kinetics of indigo carmine dye, thymol blue [32], aniline blue [33], methylene blue [34], xylenol orange [35], toludine blue [36], and acridine orange [37] involved competitive and consecutive steps with an initial slow step followed by a rapid one for depletion of dye. The rate of dye depletion increased with time as well as with [HOBr]. The dual role of the in situ generated bromine ion as an inhibitor or as an autocatalyst in the reaction mechanism has been discussed.

Reactive dyes are extensively used in the textile industry, fundamentally due to the capacity of their reactive groups to bind on textile fibers by covalent bonds formation [38]. This characteristic facilitates the interaction with the fiber and reduces energy consumption [39]. Reactive dyes represent

* Corresponding author. Tel.: +20 040 334 4352; fax: +20 040 335 0804.
E-mail address: agemeay@yahoo.com (A.H. Gemeay).

0143-7208/$ - see front matter © 2005 Elsevier Ltd. All rights reserved.
doi:10.1016/j.dyepig.2005.10.014

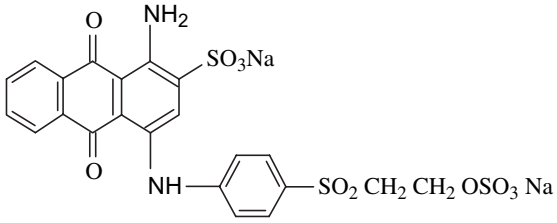

C.I. Reactive Blue 19

Scheme 1.

an important fraction of the commercialized synthetic pigments used (approximately 12% of the worldwide production) [40]. The Reactive Blue-19 (RB-19), also known as Remazol brilliant blue, is very resistant to chemical oxidation due to the fact that its aromatic anthraquinone structure is highly stabilized by resonance, Scheme 1. Photocatalytic degradation of different reactive dyes using TiO_2 revealed that the RB-19 dye was the most recalcitrant to discoloration [41]. The photocatalytic degradation of RB-19 has also been studied in the presence of TiO_2 and ZnO suspension [42,43]. ZnO showed greater degradation activity compared with TiO_2 in circulating reactor under optimized conditions.

The advantages of solid catalysts include reduced equipment corrosion, ease of product separation, less potential contamination in waste streams and recycling the catalyst. Strong acid cation-exchange resins are very versatile catalysts, which have been used commercially as solid acid catalysts in many areas [44–47]. The advantage of ion-exchange resins catalysts over other commonly used solid acid catalysts is their relatively high concentration of acid sites, and it is the factor, which makes them such effective catalysts for facile reaction.

This work is concerned with the oxidative decolorization of C. I. Reactive Blue-19 with acidic bromate solution. This point of research has been suggested to study the kinetics of the oxidation in both homogeneous and heterogeneous media. The oxidation of Reactive Blue-19 dye leads to its decolorization. This is a very important aspect in the environmental wastewater treatment of textile and dyeing fibers.

2. Experimental

2.1. Materials

All chemicals were of high grade quality and unless otherwise purification stated, they were used as received. The standard solutions and dilution were made using deionized distilled water following standard procedures. Reactive Blue (C.I. 19) disodium salt of 1-amino-2-sulfo-4-(3-sulfoxy-ethyl-sulfo-phenyl-1-yl-amino)-5,10-anthraquinone was obtained from Aldrich.

For the daily kinetic runs a stock solution of dye (10^{-3} M) was prepared. The flask containing the dye solution was wrapped in aluminum foil and stored in the dark to minimize exposure to light.

$KBrO_3$ was supplied from Merck and its initial concentration was standardized iodometrically using starch as an indicator [48]. The desired concentration of $KBrO_3$ was obtained by successive dilutions from the standard stock solution. Sodium dodecyl sulfate (SDS) and cetyltrimethylammonium bromide (CTAB) (B.D.H) were used as anionic and cationic surfactants, respectively. The critical micelle concentration (c.m.c) of the surfactants was determined by conductivity measurements both in pure water and in the reaction media.

Dowex-50W resin (8% DVB, 20–50, and 50–100 mesh size) in the hydrogen form was used as a strong acidic cation-exchanger, Dow Chemical Company. The resins were regenerated with 2 M HCl, thoroughly washed with doubly distilled H_2O and air-dried. The moisture content was determined by drying samples overnight at 110 °C and was found to be equal to 17 and 17.46% for 20–50 and 50–100 mesh, respectively. The cation-exchange capacity (CEC) of the resin was determined by titration using conventional volumetric technique and was found to be equal to 4.01 and 4.17 meq H^+/g dry resin for 20–50 and 50–100 mesh size, respectively [49].

The pH measurements were carried out with a Crison digital pH-meter model 501 equipped with a Crison glass electrode. The pH-meter was calibrated with a standard buffer solution before being used.

2.2. Kinetic measurements

The kinetic measurements were carried out spectrophotometrically using a UV/visible Shimadzu 2100S recording spectrophotometer. It is equipped with a thermo-electrically temperature controlled cell holder (TCC-260) at high accuracy over temperature 7–60 °C range. The spectrophotometer, operating via a data acquisition system, is interfaced to a computer for data storage and processing.

The kinetics of homogeneous reaction were carried out by mixing equal volumes (1 ml) of known concentrations of $KBrO_3$ and H_2SO_4 and placed in a thermostatted quartz UV cell. The reaction started by adding 1 ml of the separate thermostatted dye solution. The course of reaction was monitored by following the decay of absorbance at λ_{max} of 592 nm for RB-19. The molar extinction coefficient (ε) of the dye was determined and equal to 5336 l mol^{-1} cm^{-1}.

In a typical heterogeneous kinetic run, a number of flasks (volume 100 cm^3) containing a definite quantity of cation-exchange resin (H^+) together with doubly distilled H_2O were placed in a shaker thermostat to attain the required temperature. To each flask 1 ml of separate thermostatted dye and bromate solution were added within about 3 s by micropipette and zero time was noted at half the addition point. At regular time intervals aliquot of each flask was withdrawn and the absorbance was recorded. Generally, the dye/bromate mixture was stable for several hours without changes in the absorbance which indicates that no reaction takes place between dye and $KBrO_3$ in absence of the acidic medium (H_2SO_4 or cation-exchange resins).

3. Results and discussion

In the present study the oxidizing property of the acidified $KBrO_3$ was considered as a tool for color removal of organic

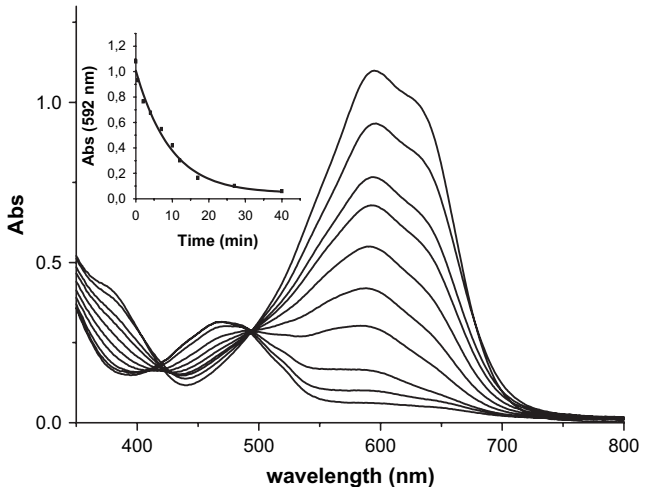

Fig. 1. Absorption spectra of the reaction of RB-19 of 1.9×10^{-4} M with $[BrO_3^-] = 0.12$ M in the presence of 0.026 M H_2SO_4 at 30 °C. The inset shows the changes of absorbance at $\lambda_{max} = 592$ nm with time.

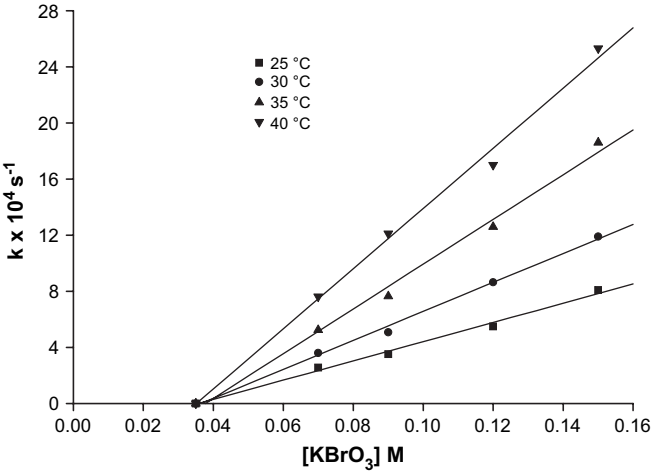

Fig. 3. Representation of the relationship between rate constant and $[BrO_3^-]$ for the reaction of $[RB\text{-}19] = 1.9 \times 10^{-4}$ M with different $[BrO_3^-]$ in the presence of 0.026 M H_2SO_4 at different temperatures.

dyes in the industrial wastewater stream. The comparison between the homogeneous and heterogeneous acid-catalyzed BrO_3^- reactions is also one of the objectives of the present work.

When RB-19 was added to the acid-free $KBrO_3$ solution no changes in the absorbance spectra have been observed. The reaction was initiated when the dye solution was allowed to react with the acidified $KBrO_3$. The absorbance of RB-19 at $\lambda_{max} = 592$ nm decreased with time as shown in Fig. 1. The kinetic measurements were carried out under pseudo-first-order conditions, where the $[KBrO_3]$ was in excess than that of the substrate. The plot of the logarithm of absorbance vs. time according to the equation: $\ln A_t = \ln A - k_0 t$ was linear as shown in Fig. 2. This indicates the first-order kinetics of the reaction with respect to the RB concentration, where A_t is the absorbance at time intervals, A is the absorbance at $t = 0$, and k_0 is the observed rate constant.

3.1. Effect of $[KBrO_3]$

The effect of the initial concentration, $[KBrO_3]_0$, on the reaction rate was investigated at constant [RB-19], 1.9×10^{-4} M, and in the presence of 0.026 M of H_2SO_4. Fig. 3 shows the relation between rate constant and $[BrO_3^-]_0$, which indicates that the reaction follows first-order kinetics with respect to the $[KBrO_3]$. The intercept of abscissa means that no reaction takes place at $[BrO_3^-]$ below 0.035 M. This means that the concentration of the generated active species is very small and unable to oxidize the RB. It has been reported that in the system involving various acidified oxybromo species such as: $H_2BrO_3^+$, $BrO_2^\bullet$, HOBr and BrO_2^- have been characterized [37,50,51]. These species could be competed with bromate ion in the oxidation and decolorization of organic dyes.

3.2. Effect of $[H_2SO_4]$

The effect of $[H_2SO_4]$ on the reaction rate was investigated by keeping the [RB-19] and $[KBrO_3]$ constant while the concentration of the acid was varied in the $(9–52) \times 10^{-3}$ M range. Fig. 4 shows the relationship between k_0 and $[H_2SO_4]$.

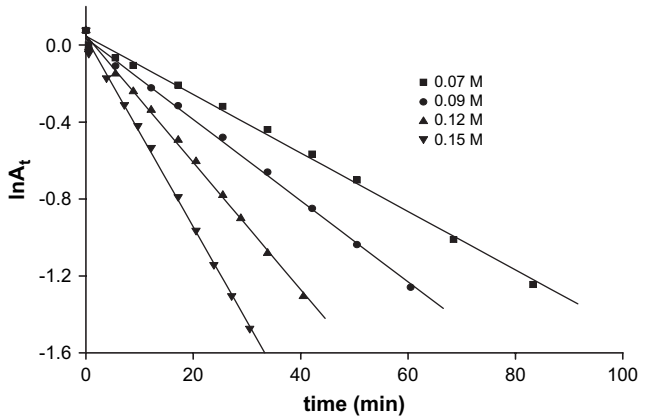

Fig. 2. Illustration of the first-order kinetic equation for the reaction of $[RB\text{-}19] = 1.9 \times 10^{-4}$ M with different $[BrO_3^-]$ in the presence of 0.026 M H_2SO_4 at 35 °C.

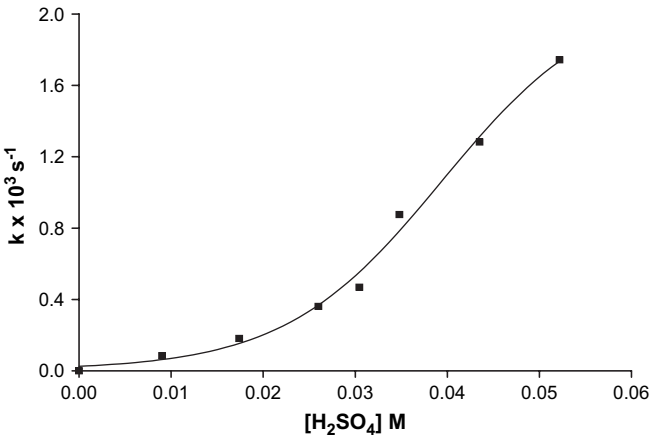

Fig. 4. Illustration of the relationship between the rate constant and the $[H_2SO_4]$ for the reaction of $[RB\text{-}19] = 1.9 \times 10^{-4}$ M with $[BrO_3^-] = 0.07$ M at 30 °C.

It is clear that the reaction rate is very slow at $[H_2SO_4]$ lower than about 0.02 M, then it is gradually increased. The order of reaction with respect to the acid concentration was determined from the plot of $\ln k$ vs $\ln [H_2SO_4]$. The slope is equal to 1.78, which is nearly equal to 2. This means that the reaction is second order with respect to $[H_2SO_4]$. Again, the slower rate obtained at lower concentrations of the acid can be attributed to the formation of the intermediates active species contributed in the oxidation reaction needed a high acid concentrations, i.e., the acid/bromate ratio should be equal to or more than 0.4 as can be seen from Fig. 4.

3.3. Effect of [RB-19]

The influence of the initial concentration of dye on the reaction rate was investigated. The $[KBrO_3]$ and $[H_2SO_4]$ were kept constant at 0.12 M and 0.026 M, respectively. Dye concentration ranged from 2×10^{-5} M to 4×10^{-4} M. Under this condition, the reaction obeyed pseudo-first-order kinetics with respect to [RB-19]. As shown in Fig. 5, increasing the [RB-19] led to a decrease in the reaction rate. This can be ascribed to the aggregation of the dye at higher concentrations [52–55]. In addition, the quantity of oxybromo species generated in the reaction are limited and depended on the $[KBrO_3]$ and $[H_2SO_4]$ which are kept constant. Therefore, the rate is decreased with increasing the [RB-19]. These results suggest that oxidative decolorization using $KBrO_3$ is likely a very efficient method to treat dye wastewater under diluted solution conditions or the method could be coupled with another preceding treatment to reduce the discharge of organic contaminants. Now, from the above-mentioned results of the individual orders, the reaction rate law can be suggested as:

$$\frac{d[\text{RB-19}]}{dt} = k[\text{RB}]\left[BrO_3^-\right][H^+]^2 \quad (1)$$

3.4. Effect of some additive ions

It is well known in the textile industry that in order to accelerate or increase the fixation of dyes onto the fibers, it is necessary to use high electrolyte concentration in dyebath to decrease the negative charged barrier between the cellulose and anionic dyes [56]. Therefore, the textile industry wastewaters are almost heavily charged with unconsumed dyes, different types of electrolytes and other chemicals. Taking into consideration that in effluents of textile dye industry, chloride and sulfate ions are naturally occurring anions ([56] and references therein), the oxidative decolorization reaction of RB-19 was monitored in the presence of NaCl and Na_2SO_4.

3.4.1. Effect of $[Cl^-]$

The influence of chloride ions, NaCl, on the reaction rate was studied. The $[Cl^-]$ was varied in the 0.003–0.2 M range, whereas the concentration of the other reactants were kept constant. A plot of k vs. [NaCl] is shown in Fig. 6, which indicates the first-order kinetics with respect $[Cl^-]$. Furthermore, the increase of k with increasing of $[Cl^-]$ indicates that the reaction is catalyzed by Cl^-. The y-axis intercept is fairly in agreement with the value of rate constant in the absence of Cl^- under comparable conditions. As shown in Fig. 6, the great increase in rate constant as the $[Cl^-]$ increased can be attributed to the formation of active chloride species such as: $Cl^{\bullet}$, Cl_2, HOCl and ClO^-, which could work as powerful oxidizing species.

3.4.2. Effect of $[Br^-]$

The effect of the initial concentrations of bromide ion as common ion effect on the reaction rate was also studied. The $[KBrO_3]$, $[H_2SO_4]$, and [RB-19] were kept constant at 0.07 M, 0.027 M, and 2×10^{-4} M, respectively, while the $[Br^-]$ was varied in 1.6×10^{-5}–1.3×10^{-4} M range. Fig. 7 shows a plot of k vs. $[Br^-]$ and illustrates that the oxidation rate of RB is greatly accelerated with increasing $[Br^-]$. This is good evidence that the $[Br^-]$ catalyzed the decolorization

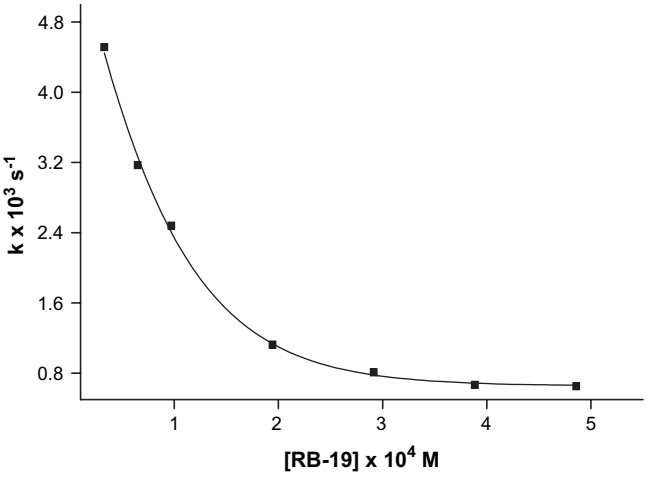

Fig. 5. The dependence of the rate constant on the [RB-19], $[BrO_3^-] = 0.07$ M, in the presence of 0.026 M H_2SO_4 at 30 °C.

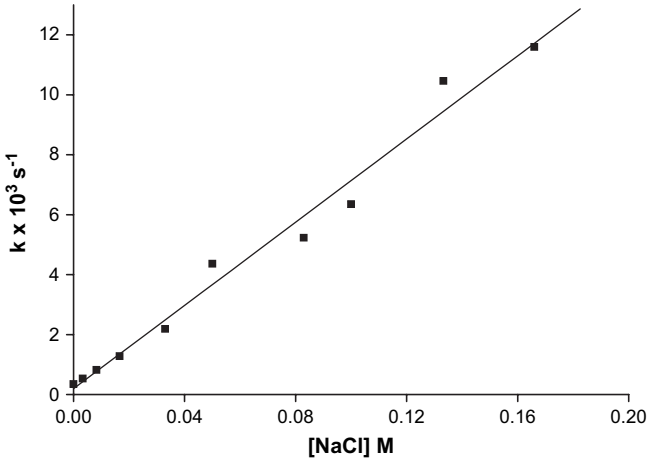

Fig. 6. Variation of the rate constant as function of [NaCl], [RB-19] = 1.9×10^{-4} M, $[BrO_3^-] = 0.07$ M, $[H_2SO_4] = 0.026$ M and at 30 °C.

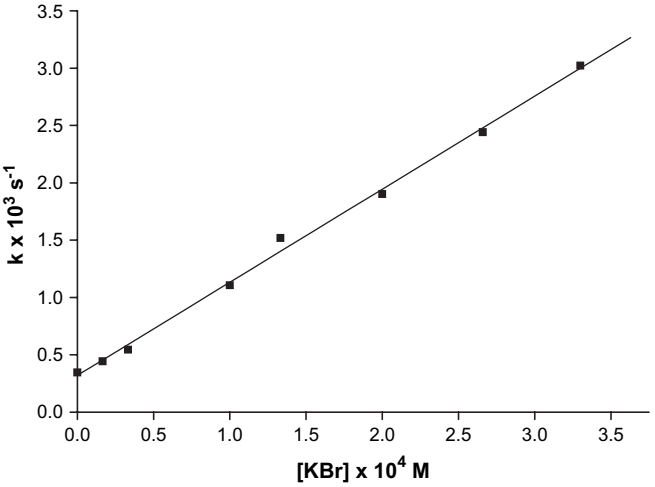

Fig. 7. Variation of the rate constant with [KBr], [RB-19] = 1.9×10^{-4} M, [BrO_3^-] = 0.07 M, [H_2SO_4] = 0.026 M at 30 °C.

of RB-19. It has been reported that the addition of [Br^-] in the reaction medium containing acidified $KBrO_3$ facilitated the generation of bromine and hypobromous acid species [32]. The intercept (0.321×10^{-2} s^{-1}) shown in Fig. 7 is fairly in agreement with the rate constant ($k = 0.346 \times 10^{-2}$ s^{-1}) determined for the reaction in absence of the bromide ions under comparable conditions. Also, Fig. 7 indicates that the order of reaction with respect to [Br^-] is one as concluded from the linearity of the relation.

3.4.3. Effect of [SO_4^{2-}]

The effect of the initial concentrations of sulfate ions was also investigated. The concentration of the reactants was held constant, while the concentration of K_2SO_4 was varied in $(0.83-8.3) \times 10^{-2}$ M range. As shown in Fig. 8, the plot of k vs. [SO_4^{2-}] exhibited a sharp decrease of the rate constant with increasing [SO_4^{2-}]. This could be ascribed to the decreasing H^+ concentration in the reaction medium through the decrease of ionization constant of H_2SO_4 with increasing [SO_4^{2-}].

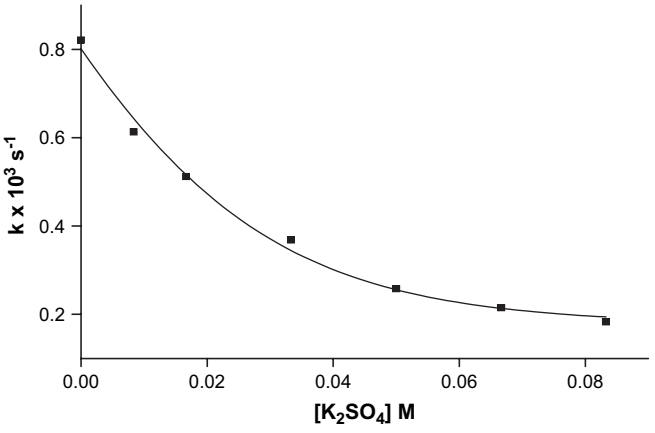

Fig. 8. The dependence of the rate constant on the [K_2SO_4], [RB-19] = 1.9×10^{-4} M, [BrO_3^-] = 0.12 M, [H_2SO_4] = 0.026 M and at 30 °C.

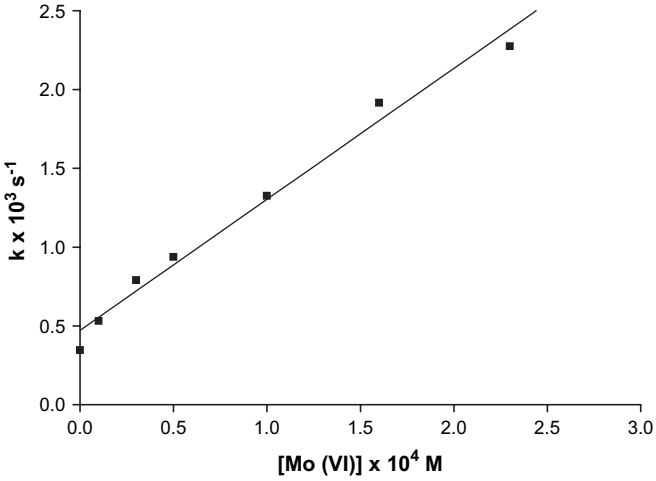

Fig. 9. Variation of the rate constant with the [$(NH_4)_6$ Mo_7O_{24} $\cdot 4H_2O$] donated as [Mo(IV)], [RB-19] = 1.9×10^{-4} M, [BrO_3^-] = 0.07 M, [H_2SO_4] = 0.026 M, at 30 °C.

3.4.4. Effect of Mo(VI)

The influence of the Mo(VI) ions ($(NH_4)_2Mo_2O_7$) was also studied. The concentration of the reactants were held constant while the [Mo(VI)] was changed in $(0.1-2.3) \times 10^{-4}$ M range. As shown in Fig. 9, a plot of k vs. [Mo(VI)], the linear relation confirms the first-order kinetics with respect to the [Mo(VI)]. The intercept represents the contribution of the uncatalyzed path of the reaction The catalytic effect of Mo(VI) ion on the reactions of acidic BrO_3^- with different substrates was reported elsewhere [50,57]. Thus, the rate equation can be written down in the following form:

$$-\frac{d[\text{RB-19}]}{dt} = k_{\text{uncat}}[\text{RB-19}]\left[BrO_3^-\right][H^+]^2 + k_{\text{cat}}[\text{RB-19}]\left[BrO_3^-\right][H^+]^2[\text{Mo(VI)}] \quad (2)$$

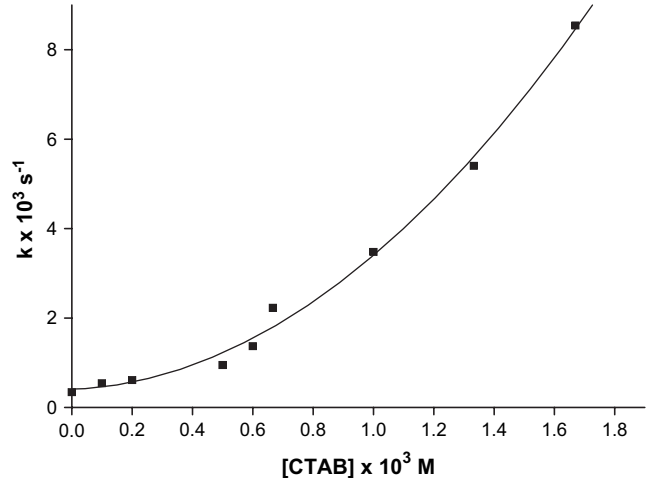

Fig. 10. Variation of the rate constant with the [CTAB], [RB-19] = 231.9×10^{-4} M, [BrO_3^-] = 0.07 M, [H_2SO_4] = 0.026 M, at 30 °C.

3.5. Effect of surfactants

The influence of both the anionic and cationic surfactants on the reaction rate was investigated. When the anionic surfactant, sodium dodecyl sulfate (SDS) was added to the reaction medium no reaction has been observed. This effect can be quantitatively explained on the basis of ion-exchange model. The presence of SDS decreases the H^+ concentration through their exchanging with Na^+ counter ions. The same behavior has been found elsewhere [58]. On the other hand, when the cationic surfactant cetyltrimethylammonium bromide (CTAB) was added to the reaction medium an enhancement of the reaction rate has been observed. As shown in Fig. 10 increasing the [CTAB] led to an increase in the rate constant. This effect can be quantitatively explained on basis of the ion exchange model, i.e., the increase of CTAB concentration led to an increase of the bromide ion concentration, which could be acted as a catalyst for the decolorization reaction [58].

3.6. Heterogeneous reaction

When RB-19 was allowed to react with BrO_3^- in the presence of a definite amount of cation-exchange resin (H^+-form) the absorbance declined exponentially with time. The amount of dry cation-exchange resin (8%, DVB, 20–50 mesh) sufficiently required to achieve the reaction was 0.08 g, whereby the [BrO_3^-] was 100 times in excess of that of [RB-19] under pseudo-first-order conditions. The linear plot of Fig. 11 confirms the zero-order kinetics of the reaction.

The effect of [$KBrO_3$] on the reaction was also examined by keeping the concentration of the reactants constant, whereas that of $KBrO_3$ was varied. Fig. 12 shows the dependence of the rate constant k (per gram of dry resin) on the initial concentration of $[KBrO_3]_0$. This indicates the first-order kinetics with respect to the oxidant concentration. The intercept with the abscissa (0.03 M) indicates that reaction did not take place in the presence of oxidant concentration lower than 0.03 M. This value is almost the same as that found for the homogeneous catalyzed reaction. Taking into account that the [H^+] of the homogeneous and heterogeneous catalyzed reactions are 0.026 M and 0.32×10^{-3} M, respectively. This indicates that although the [H^+] in the heterogeneous reaction is very small compared with that in homogeneous one, yet it exhibited a similar activity. The conclusion could be withdrawn that the adsorption of RB-19 on cation-exchange resin surface might be playing a role in the decolorization reaction.

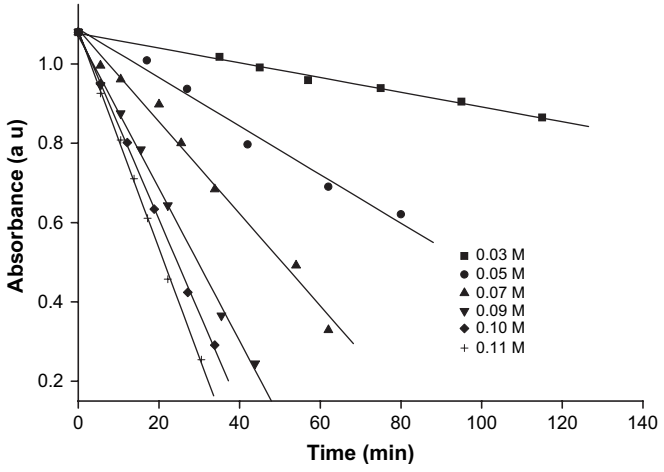

Fig. 11. Zero-order plot for the oxidative reaction of RB-19 of 1.9×10^{-4} M with different [BrO_3^-] in the presence of 0.08 g of ion exchange resin, Dowex-50W, 8% DVB (20–50 mesh) (H^+-form) at 30 °C.

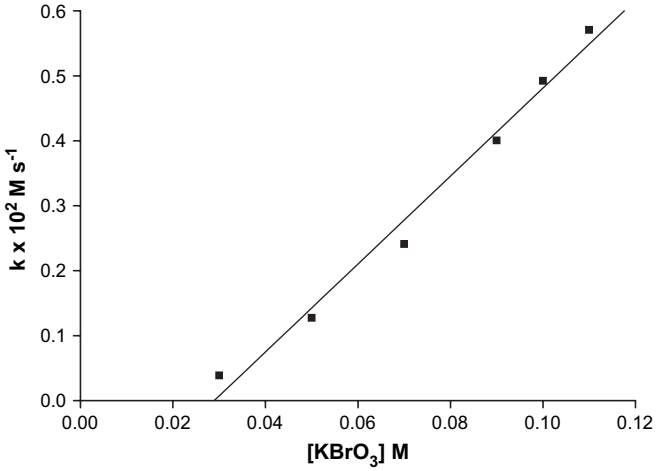

Fig. 12. Variation of the rate constant with [BrO_3^-] under the reaction conditions mentioned in Fig. 11.

The effect of the mesh size of cation-exchange resin on the reaction rate was also considered by employing the cation-exchange resin of 8% DVB (50–100 mesh). The reaction also exhibited zero-order kinetics with respect to [RB-19]. It was found that the reaction rate is almost the same as in the case of 20–50 mesh under the same working conditions. This similarity of reaction rate could be attributed to the little difference of the mesh size of the resins. Moreover, the cation-exchange capacity of resins may play a considerable role. The cation-exchange capacities are 4.01 and 4.17 meq H^+/g dry resin for the resin of 20–50 and 50–100 meshes, respectively.

3.7. Effect of temperature

The kinetic measurements of both the homogeneous and heterogeneous acid-catalyzed reactions were carried out at various temperatures in 25–40 °C range. A plot of Arrhenius equation was applied and the activation energy, E was deduced. The other activation parameters were determined and are listed in Tables 1 and 2. It is clear that the enthalpy is

Table 1
Rate constants and the activation parameters for the reaction of RB-19 of 1.9×10^{-4} M with bromate ion of 0.07 M in the presence of 0.026 M of H_2SO_4

Temp (°C)	$k \times 10^4$ (s^{-1})	E (kJ/mol)	$\Delta H^{\#}$ (kJ/mol)	$\Delta G^{\#}$ (kJ/mol)	$\Delta S^{\#}$ (J mol^{-1} deg^{-1})
25	2.6	67.3	65.3	83.9	−70.0
30	3.6				
35	5.2				
40	7.4				

Table 2
The rate constant and the activation parameters for the reaction of RB-19 (1.9×10^{-4} M) with bromate ion (0.07 M) in the presence of 0.08 g of air-dried Dowex-50W (8% DVB, 20–50, and 50–100 mesh size) cation-exchange resin (H^+-form)

Mesh size	Temp. (°C)	$k \times 10^2$ ($M\ s^{-1}$)	E ($kJ\ mol^{-1}$)	$\Delta H^{\#}$ ($kJ\ mol^{-1}$)	$\Delta G^{\#}$ ($kJ\ mol^{-1}$)	$\Delta S^{\#}$ ($J\ mol^{-1}\ K^{-1}$)
50–100	25	0.18	49.80	47.20	89.70	140.0
	30	0.26				
	35	0.36				
	40	0.47				
20–50	25	0.19	48.10	45.60	89.60	150.0
	30	0.26				
	35	0.36				
	40	0.49				

greater for the faster system (homogeneous), which indicates that the decolorization reaction is entropy controlled [55].

3.8. Reaction mechanism

Based on the above results and discussion, the mechanism of the oxidation of RB-19 by acidified bromate can be proposed. Eqs. (3) and (4) represent the chemistry of the bromate ion in acid solution [59,60], which may be followed by the reaction of RB-19 with $H_2BrO_3^+$ ion in the rate-determining step, Eq. (5)

$$H^+ + BrO_3^- \overset{K_1}{\leftrightarrow} HBrO_3 \tag{3}$$

$$H^+ + HBrO_3 \overset{K_2}{\leftrightarrow} H_2BrO_3^+ \tag{4}$$

$$\text{RB-19} + H_2BrO_3^+ \xrightarrow[\text{slow}]{k_3} \text{product} \tag{5}$$

Thus, the rate equation can be written as:

$$V = k_3[\text{RB-19}]\left[H_2BrO_3^+\right] \tag{6}$$

The equilibrium constants in Eqs. (3) and (4) can be represented as:

$$K_1 = [HBrO_3]/[H^+][BrO_3^-] \tag{7}$$

$$K_2 = \frac{\left[H_2BrO_3^+\right]}{[H^+][HBrO_3]} \tag{8}$$

Thus,

$$[HBrO_3] = K_1[H^+]\left[BrO_3^-\right] \tag{9}$$

and

$$\left[H_2BrO_3^+\right] = K_2[H^+][HBrO_3] \tag{10}$$

By substituting Eq. (10) in Eq. (6) we get:

$$V = k_3K_2[\text{RB-19}][H^+][HBrO_3] \tag{11}$$

Also by substituting Eq. (9) in Eq. (11) we get:

$$V = K_1K_2k_3[\text{RB-19}][H^+]^2\left[BrO_3^-\right] \tag{12}$$

or

$$V = k_t[\text{RB-19}]\left[BrO_3^-\right][H^+]^2 \tag{13}$$

where, $k_t = K_1K_2k_3$.

Eq. (13) is in good agreement with the obtained results since the reaction exhibited first order with respect to the concentrations of RB-19 and bromate and second order with respect to $[H^+]$.

4. Conclusions

The oxidative decolorization of Reactive Blue-19 dye by potassium bromate acidified with H_2SO_4 (homogeneous medium) or cation-exchange resin (heterogeneous medium) has been achieved. The reaction followed first-order kinetics in homogeneous medium while in heterogeneous medium zero-order kinetics was followed. The decolorization rate was enhanced with increasing the concentrations of, BrO_3^-, H_2SO_4, Br^-, Cl^-, Mo(VI), and CTAB, while it decreases with increasing the [RB-19] and $[SO_4^-]$, and independent of the concentration of anionic surfactant (SDS). Although, the homogeneous system gave a higher rate compared with heterogeneous one, it is recommended to use the heterogeneous system for the treatment of wastewater containing Reactive Blue-19 dye to minimize the addition of chemicals.

References

[1] Qin J, Zhang Q, Chuang KT. Appl Catal B 2001;29:115.
[2] Fujitani T, Nakamura. Appl Catal A 2000;191:111.
[3] Li XZ, Zhao YG. Water Sci Technol 1999;39:249.
[4] Lopez A, Ricco G, Ciannarella R, Rozzi A, Dipinto AC, Passino R. Water Sci Technol 1999;40:99.
[5] Pak D, Chang W. Water Sci Technol 1999;40:115.
[6] Chu W, Ma CW. Water Res 2000;34:3153.
[7] Gregory P, Stead CV. J Soc Dyers Colour 1978;94:402.
[8] Bredereck K, Schumacher C. Dyes Pigments 1993;21:45.
[9] Omura T, Kayane Y, Tezuka Y. Dyes Pigments 1992;20:227.
[10] Omura T. Dyes Pigments 1992;23:179.
[11] Phillips D, Duncan M, Jenkins E, Bevan G, Lloyd J, Hoffmeister J. J Soc Dyers Colour 1996;112:287.
[12] Oakes J, Grotton P, Clark R, Wilkes I. J Chem Soc Perkin Trans 2 1998:2569.
[13] Oakes J, Grotton P. J Chem Soc Perkin Trans 2 1998:1857.
[14] Oakes J, Grotton P, Gordan Smith T. Dyes Pigments 2000;46:169.
[15] Davies DM, Moozychine AU. J Chem Soc Perkin Trans 2 2000:1495.
[16] Salem IA, El-Maazawi M. Z Phys Chemie 2001;215:623.
[17] Arslan I, Balcioglu IA. Dyes Pigments 2000;46:169.
[18] Herrera F, Lopez A, Mascolo G, Albers P, Kiwi J. Appl Catal B 2001;29:147.
[19] Joseph JM, Destaillates H, Hhung HM, Haffmann MR. J Phys Chem A 2000;301:104.
[20] Tokuda J, Oura R, Iwasaki T, Takeuchi Y, Kashiwada A, Nango M. J Soc Dyers Colour 2000;116:42.
[21] Salem IA. Appl Catal B 2001;28:153.
[22] Salem IA. Chemosphere 2001;44:1109.

[23] Fukushima M, Tatsumi K, Morimoto K. Environ Sci Technol 2000;34: 2006.
[24] Li L, Wang A, He P, Fang Y, Fresenius. J Anal Chem 2000;367:649.
[25] Yang TCK, Wang SF, Tsai SHY, Lin SY. Appl Catal B 2001;30:293.
[26] Arslan I, Balcioglu IA. Color Technol 2001;117:38.
[27] Galindo C, Jacques P, Kalt A. J Photochem Photobiol A 2000;130:35.
[28] Liu G, Li X, Zhao J, Horikoshi S, Hidaka H. J Mol Catal A 2000; 153:221.
[29] Zhang XY, Field RJ. J Phys Chem 1990;94:1224.
[30] Jonnalagadda SB, Chinake CR, Simoyi RH. J Phys Chem 1996; 100:13530.
[31] Jonnalagadda SB. Pure Appl Chem 1998;70:645.
[32] Jonnalagadda SB, Salem MA. Phys Chem Chem Phys 1999;1:821.
[33] Jonnalagadda SB, Simoyi RH, Muthkia GK. J Chem Soc Perkin Trans 2 1988;7:1111.
[34] Muthkia GK, Jonnalagadda SB. J Phys Chem 1989;93:4751.
[35] Ensafi AA, Amini ME, Mazloum M. Indian J Chem 1997;36A:626.
[36] Jonnalagadda SB, Muthakia GK. J Chem Soc Perkin Trans 2 1987;7: 1539.
[37] Swawunyama P, Jonnalagadda SB. J Phys Org Chem 1995;8:175.
[38] Weber J, Stickny VC. Water Res 1993;27:63–7.
[39] Camp R, Sturrock PE. Water Res 1990;24:1275–8.
[40] Scharmm KW, Hirsch M, Twelve R, Hutzinger O. Water Res 1988;23: 1043–5.
[41] Lizama C, Yeber MC, Freer J, Baeza J, Mansilla HD. Water Sci Technol 2001;44:197.
[42] Lizama C, Freer J, Baeza J, Mansilla HD. Catal Today 2002;76:235–46.
[43] Pelegrini R, Peralta-Zamora P, de Andrade AR, Reyes J, Duran N. Appl Catal B Environ 1999;22:83–90.
[44] Hodge P, Sherrington DS. Synthesis and separations using functionalised polymers. Chichester: Wiley; 1988.
[45] Anasthas HM, Gaikar VG. React Funct Polym 2001;47:23.
[46] Rhodes CN, Brown DR, Plant S, Dale JA. React Funct Polym 1999; 40:187.
[47] Girolamo MD, Marchionna M. J Mol Catal A 2001;177:33.
[48] Sullivan JC, Thompson RC. Inorg Chem 1979;18:2375.
[49] Musante RL, Grau RJ, Baltanas MA. Appl Catal A 2000;197:165.
[50] Orban M, Dekepper F, Epstein IR. J Am Chem Soc 1982;104:2657.
[51] Foersterting H, Varga M. J Phys Chem 1993;97:7932.
[52] Dan P, Willner I, Dixit NS, Mackay RA. J Chem Soc Perkin Trans 2 1984:455.
[53] Gemeay Ali H, Mansour Ikhlas A, El-Sharkawy Rehab G, Zaki Ahmed B. J Mol Catal A Chem 2003;193:109–20.
[54] Gemeay Ali H. Dyes Pigments 2002;54:201–12.
[55] Gemeay Ali H, Mansour Ikhlas A, El-Sharkawy Rehab G, Zaki Ahmed B. J Chem Technol Biotechnol 2004;79:85–96.
[56] Carneiro PA, Osugi ME, Sene JJ, Anderson MA, Zanoni MVB. Electrochim Acta 2004;49:3807–20.
[57] Bazsa G, Fabian I. J Chem Soc Dalton Trans 1986:2675.
[58] Barton AFB, Loo Boon-Hian. J Chem Soc A 1971:3032.
[59] Dominguez A, Iglesias E. Langmuir 1998;14(10):2677.
[60] Herbine P, Field RJ. J Phys Chem 1980;84:1330.